Implementation and position control performance of a position-sensorless IPM motor drive system based on magnetic saliency

Satoshi Ogasawara
Okayama University

Hirofumi Akagi
Okayama University

Implementation and Position Control Performance of a Position-Sensorless IPM Motor Drive System Based on Magnetic Saliency

Satoshi Ogasawara, *Senior Member, IEEE*, and Hirofumi Akagi, *Fellow, IEEE*
Okayama University
3-1-1 Tsushima-Naka, Okayama, 700 JAPAN

***Abstract*—This paper describes position-sensorless control of an interior permanent magnet synchronous motor (IPM motor), which is characterized by real-time position estimation based on magnetic saliency. The real-time estimation algorithm detects motor current harmonics and determines the inductance matrix including rotor position information. An experimental system consisting of an IPM motor and a voltage-source PWM inverter has been implemented and tested to confirm the effectiveness and versatility of the approach. Some experimental results show that the experimental system has the function of electrically locking the loaded motor, along with a position response of 20 rad/s and a settling time of 300 ms.**

I. Introduction

The improvement of permanent magnet materials is widening the application of permanent magnet synchronous motors (PM motors). Since a PM motor is a three-phase synchronous machine, knowledge of rotor position is indispensable for controlling it quickly. For this reason, a position sensor such as a rotary encoder is usually used in a PM motor drive system. From the viewpoints of reliability, robustness and cost, much attention has been paid to position-sensorless drives that can control position, speed and/or torque of a PM motor without any shaft-mounted position sensors. Principles of position estimation can be classified into two techniques based on back electromotive force and on magnetic saliency. Position estimation based on back electromotive force has good characteristics in middle- and high-speed ranges [1], [2]. However, since the amplitude of the back electromotive force is in proportion to the rotating speed, position estimation at a standstill and at low speed is difficult. On the other hand, position estimation based on magnetic saliency is promising for next-generation sensorless drives, because it can estimate the rotor position at any rotor speed [3]–[6]. Although some position estimation methods based on magnetic saliency have been proposed, they need to inject an extra signal into the motor current or voltage.

This paper deals with position control of a position-sensorless PM motor drive. An approach to real-time position estimation based on magnetic saliency is introduced to an interior permanent magnet synchronous motor (IPM motor). The approach proposed by the authors [7] is characterized by a real-time estimation algorithm: It determines the inductance matrix including rotor position information from current harmonics produced by switching operations of an inverter driving the IPM motor, and then estimates the rotor position every period of pulse-width modulation (PWM). Position estimation without any special signal injection is achieved with a satisfactory response and accuracy even at a standstill and at low speed. An experimental system consisting of an IPM motor (100 W) and a voltage-source PWM inverter has been constructed and tested to confirm the effectiveness and versatility of the approach. The IPM motor has a magnetic saliency of the q-axis inductance being larger than the d-axis inductance. As a result, experiments show that the constructed system provides a position response of 20 rad/s and a settling time of 300 ms. Furthermore, it is demonstrated that the experimental system can electrically lock the loaded motor shaft, providing stiffness during positioning.

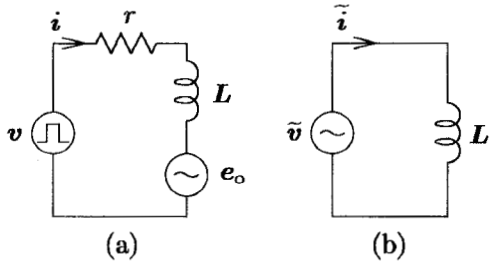

Fig. 1. Equivalent circuit of an IPM motor.

II. Position Estimation Based on Magnetic Saliency

A. Principle of Estimation

Fig. 1(a) shows an equivalent circuit of an IPM motor. Here, $\boldsymbol{v}$, $\boldsymbol{i}$ and $\boldsymbol{e}_0$ are motor voltage and current vectors, and a back electromagnetic force vector on the stator coordinates, respectively. The inductance matrix is represented by

$$\boldsymbol{L} = \begin{bmatrix} L_0 + L_1 \cos 2\theta & L_1 \sin 2\theta \\ L_1 \sin 2\theta & L_0 - L_1 \cos 2\theta \end{bmatrix} \tag{1}$$

$$L_0 = \frac{L_d + L_q}{2}, \qquad L_1 = \frac{L_d - L_q}{2} \tag{2}$$

and it contains rotor position θ.

0-7803-4067-1/97/$10.00 © 1997 IEEE.

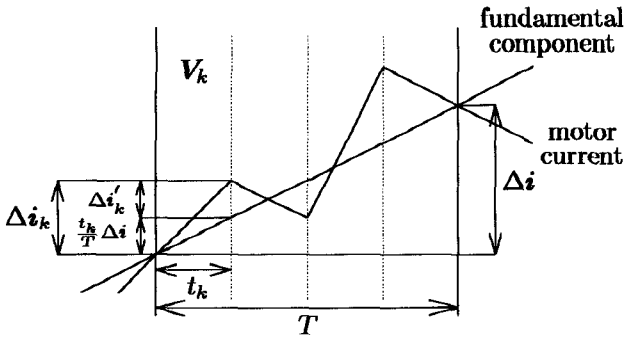

Fig. 2. Motor current waveform.

When the IPM motor is driven by a voltage source PWM inverter, the motor current contains a small amount of harmonic current. The voltage and current vectors can be separated into the fundamental and harmonic components as follows:

$$\boldsymbol{v} = \bar{\boldsymbol{v}} + \tilde{\boldsymbol{v}} \tag{3}$$

$$\boldsymbol{i} = \bar{\boldsymbol{i}} + \tilde{\boldsymbol{i}}. \tag{4}$$

Because the effect of resistor r on a voltage drop can be disregared for the harmonic component, Fig. 1(a) can be approximated by Fig. 1(b), that is,

$$\tilde{\boldsymbol{v}} = \boldsymbol{L}\frac{d\tilde{\boldsymbol{i}}}{dt}. \tag{5}$$

The above equation indicates that the inductance matrix can be calculated from the harmonic components of the motor voltage and current vectors, so that θ can be estimated [8][9].

B. Extraction of Harmonic Voltage and Current Vectors

The PWM inverter has the capability of producing an output voltage vector by selecting discrete voltage vectors in a modulation period [10]. The average voltage vector is

$$\boldsymbol{e} = \sum \zeta_k \boldsymbol{V}_k \tag{6}$$

where ζ_k means a time ratio of $\boldsymbol{V}_k$ with respect to the modulation period:

$$\zeta_k = \frac{t_k}{T}. \tag{7}$$

Therefore the harmonic voltage vector is equal to a difference between the inverter output voltage vector and the average output voltage vector:

$$\boldsymbol{V}_k{}' = \boldsymbol{V}_k - \boldsymbol{e}. \tag{8}$$

On the other hand, invoking the approximation of (5) implies that the motor current changes linearly as shown in Fig. 2. Since the motor current includes both the fundamental and harmonic components, the two components should be separated from each other. The current variation for the modulation period is shown by

$$\Delta\boldsymbol{i} = \sum \Delta\boldsymbol{i}_k \tag{9}$$

where $\Delta\boldsymbol{i}_0, \cdots, \Delta\boldsymbol{i}_7$ are the current variations for the intervals of $t_0, \cdots, t_7$, respectively. Assuming that the fundamental component changes linearly in the modulation period, the harmonic component of the current variation can be separated by the following equation:

$$\Delta\boldsymbol{i}_k{}' = \Delta\boldsymbol{i}_k - \zeta_k \Delta\boldsymbol{i}. \tag{10}$$

As a result, we can extract only their harmonic components from the voltage and current vectors.

C. Estimation of Inductance Matrix and Rotor Position

From (5), a relationship between the harmonic components of the voltage vector and the current variation vector is given by

$$\boldsymbol{L}\Delta\boldsymbol{i}_k{}' = \boldsymbol{V}_k{}' t_k. \tag{11}$$

Lumping the above equations together over the modulation period gives the following equation:

$$\boldsymbol{L}\left[\begin{array}{cccc} \Delta\boldsymbol{i}_0{}' & \Delta\boldsymbol{i}_1{}' & \cdots & \Delta\boldsymbol{i}_7{}' \end{array}\right] = \left[\begin{array}{cccc} \boldsymbol{V}_0{}' t_0 & \boldsymbol{V}_1{}' t_1 & \cdots & \boldsymbol{V}_7{}' t_7 \end{array}\right]. \tag{12}$$

The transposed equation is

$$\left[\begin{array}{c} \Delta\boldsymbol{i}_0{}'^{\mathrm{T}} \\ \Delta\boldsymbol{i}_1{}'^{\mathrm{T}} \\ \vdots \\ \Delta\boldsymbol{i}_7{}'^{\mathrm{T}} \end{array}\right] \boldsymbol{L}^{\mathrm{T}} = \left[\begin{array}{c} \boldsymbol{V}_0{}'^{\mathrm{T}} t_0 \\ \boldsymbol{V}_1{}'^{\mathrm{T}} t_1 \\ \vdots \\ \boldsymbol{V}_7{}'^{\mathrm{T}} t_7 \end{array}\right]. \tag{13}$$

Therefore, the inductance matrix can be calculated as follows:

$$\begin{aligned} \boldsymbol{L}^{\mathrm{T}} &= \left[\begin{array}{c} \Delta\boldsymbol{i}_0{}'^{\mathrm{T}} \\ \Delta\boldsymbol{i}_1{}'^{\mathrm{T}} \\ \vdots \\ \Delta\boldsymbol{i}_7{}'^{\mathrm{T}} \end{array}\right]^{\mathrm{LM}} \left[\begin{array}{c} \boldsymbol{V}_0{}'^{\mathrm{T}} t_0 \\ \boldsymbol{V}_1{}'^{\mathrm{T}} t_1 \\ \vdots \\ \boldsymbol{V}_7{}'^{\mathrm{T}} t_7 \end{array}\right] \\ &= \left[\begin{array}{cc} L_{11} & L_{12} \\ L_{21} & L_{22} \end{array}\right]^{\mathrm{T}} \\ &= \left[\begin{array}{cc} L_0 + L_1\cos 2\theta & L_1 \sin 2\theta \\ L_1 \sin 2\theta & L_0 - L_1 \cos 2\theta \end{array}\right]. \end{aligned} \tag{14}$$

Here, the "LM" in the above equation is the *left pseudo inverse* operator[11], and it performs the following calculation:

$$\boldsymbol{H}^{\mathrm{LM}} = \left(\boldsymbol{H}^{\mathrm{T}}\boldsymbol{H}\right)^{-1}\boldsymbol{H}^{\mathrm{T}}. \tag{15}$$

Thus the rotor position can be calculated from the inductance matrix:

$$2\theta = \tan^{-1}\frac{L_{12} + L_{21}}{L_{11} - L_{22}}. \tag{16}$$

Note that the left hand of (16) is not θ but 2θ. It would be possible to distinguish the polarity of the rotor magnetic pole by means of another technique based on magnetic saturation [3].

III. Modification of PWM

The inverse matrix of $\boldsymbol{H}^{\mathrm{T}}\boldsymbol{H}$ must be existent, otherwise we can not calculate the left pseudo inverse in (14). If all of $\boldsymbol{\Delta i}_k$ are linearly dependent, no inverse matrix exists because the determinant of the matrix is equal to zero, i.e. $\det(\boldsymbol{H}^{\mathrm{T}}\boldsymbol{H}) = 0$. Therefore, a conventional PWM scheme should be modified by using redundant voltage vectors, so that all of $\boldsymbol{\Delta i}_k$ are not linearly dependent vectors [7].

The following equations represent an average voltage vector during the modulation period:

$$\boldsymbol{e} = \sum s_k \zeta_k \boldsymbol{V}_k \tag{17}$$

$$\sum s_k \zeta_k = 1. \tag{18}$$

Here, s_k, taking a value of either 1 or 0 during the modulation period, indicates whether or not $\boldsymbol{V}_k$ is selected as an output vector. Lumping the equations together gives the following equation:

$$\begin{bmatrix} e_\alpha \\ e_\beta \\ 1 \end{bmatrix} = \begin{bmatrix} s_0 V_{0\alpha} & s_1 V_{1\alpha} & \cdots & s_7 V_{7\alpha} \\ s_0 V_{0\beta} & s_1 V_{1\beta} & \cdots & s_7 V_{7\beta} \\ s_0 & s_1 & \cdots & s_7 \end{bmatrix} \begin{bmatrix} \zeta_0 \\ \zeta_1 \\ \vdots \\ \zeta_7 \end{bmatrix}. \tag{19}$$

In the above equation, ζ_k has to be decided so that the PWM inverter outputs the average voltage vector $\boldsymbol{e}$ during the modulation period. No general solution to (19) exists because the number of unknown variables is more than the number of equations. However, introducing a *right pseudo inverse* matrix[11] enables us to solve ζ_k as follows:

$$\begin{bmatrix} \zeta_0 \\ \zeta_1 \\ \vdots \\ \zeta_7 \end{bmatrix} = \begin{bmatrix} s_0 V_{0\alpha} & s_1 V_{1\alpha} & \cdots & s_7 V_{7\alpha} \\ s_0 V_{0\beta} & s_1 V_{1\beta} & \cdots & s_7 V_{7\beta} \\ s_0 & s_1 & \cdots & s_7 \end{bmatrix}^{\mathrm{RM}} \begin{bmatrix} e_\alpha \\ e_\beta \\ 1 \end{bmatrix} \tag{20}$$

where

$$\boldsymbol{F}^{\mathrm{RM}} = \boldsymbol{F}^{\mathrm{T}} \left(\boldsymbol{F}\boldsymbol{F}^{\mathrm{T}} \right)^{-1}. \tag{21}$$

As a result of the calculation, we can decide some PWM patterns under any combination of $\boldsymbol{V}_k$ during the modulation period.

Fig. 3 shows a PWM pattern suitable for estimation in a low speed range. This PWM pattern is applied to the experimental system implemented in this paper. Note that the inverter selects neither $\boldsymbol{V}_1$ nor $\boldsymbol{V}_7$. The sequence is scheduled so that the trajectory of the harmonic current vector starts from the origin at the beginning of the modulation period and returns to the origin at the end. Since all of $\boldsymbol{\Delta i}'_k$ are not linearly dependent, the position estimation can be performed even at a standstill.

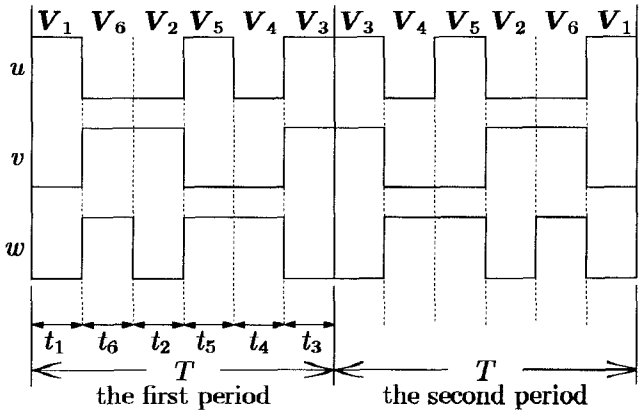

(a) PWM pattern

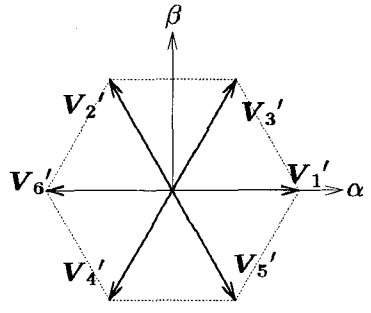

(b) Harmonic voltage vectors

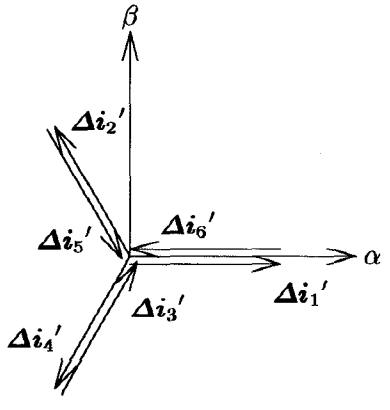

(c) Trajectory of harmonic current vector

Fig. 3. PWM scheme using redundant voltage vectors. The average voltage vector exists on the origin of the α-β coordinate.

IV. Experimental System

A. System Configuration

Fig. 4 shows the configuration of an experimental system. The controller surrounded by a broken line consists

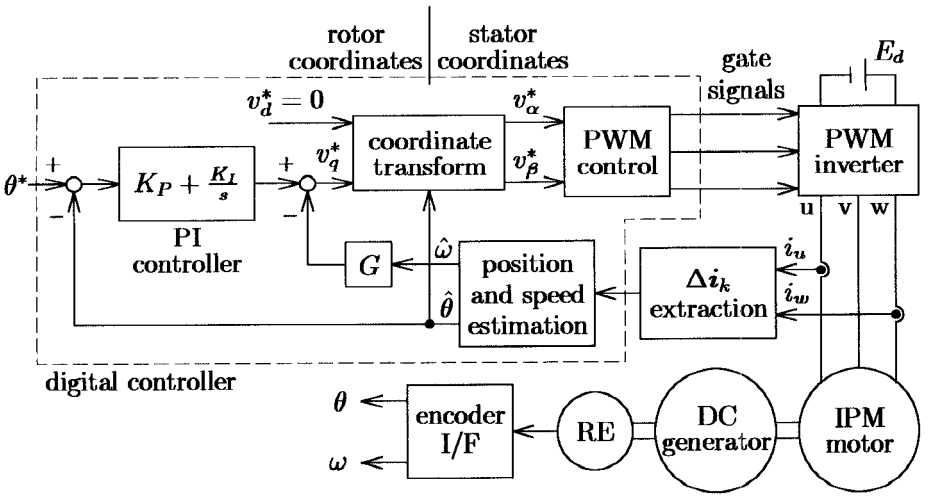

Fig. 4. System configuration

of a digital circuit using a digital signal processor (ADSP-2101) and a microprocessor (V40). Two current sensors detect u-phase and w-phase motor currents, and then the current variation vector $\Delta \boldsymbol{i}_k$ is extracted. Estimated rotor position $\hat{\theta}$ is obtained from $\Delta \boldsymbol{i}_k$ and PWM signals, based on the approach shown in section II. In addition, estimated rotor speed $\hat{\omega}$ is given by the difference in the estimated rotor position with respect to time.

This system constitutes a position-control loop feeding back the estimated position $\hat{\theta}$ to the q-axis voltage. Moreover, a speed minor loop of the estimated speed $\hat{\omega}$ is added for the purpose of improving stability of position control [12]. Here, for the sake of simplicity, there is no current control loop. The PI controller and the speed minor loop give the q-axis voltage reference v_q^*, while the d-axis voltage reference v_d^* is always zero. In addition, a coordinate transformer relying on the estimated rotor position converts v_d^* and v_q^* on the rotor coordinates to v_α^* and v_β^* on the stator coordinates. Gate signals of the voltage-source PWM inverter are generated, as shown in Fig. 3. A PWM period of T=333 μs corresponds to a carrier frequency of 1.5 kHz in a conventional sinusoidal PWM inverter in which three-phase sinusoidal reference voltages are compared with a triangular wave. In this system, however, the average switching frequency is 5.5 kHz because several switchings occur during T, period as shown in Fig. 3. The DSP can calculate the estimated rotor position and the PWM pattern within 20 μs and 50 μs, respectively.

Table I shows motor and inverter parameters of the experimental system. The q-axis inductance is larger than the d-axis inductance, which stems from a rotor structure in which the magnets are buried inside the rotor. The IPM motor is mechanically coupled with a dc generator used as a load. Actual position and speed are detected by a rotary encoder (RE), but these signals are not used in the position control system.

TABLE I

MOTOR AND INVERTER PARAMETERS OF EXPERIMENTAL SYSTEM.

number of poles		4	
armature resistance	r	15	Ω
d-axis inductance	L_d	125	mH
q-axis inductance	L_q	206	mH
rated power		100	W
rated speed		1500	rpm
modulation period	T	333	μs
dc-link voltage	E_d	280	V

B. Extraction of Δi_k

If A/D converters directly converted the detected current signals to digital current signals, high resolution would be required for the A/D converters, in order to meet required accuracy in difference calculation for extracting $\Delta \boldsymbol{i}_k$. Fig. 5 shows an actual circuit configuration for extracting $\Delta \boldsymbol{i}_k$. Two AC-CTs devote their role only to calculating $\Delta \boldsymbol{i}_k$, because there is no current minor loop added. The detected three-phase motor currents are transformed to two-phase motor currents on the stator coordinates, and fourteen sample & hold (S/H) amplifiers receive them. Seven S/H signals are generated from PWM signals in the first period of Fig. 3 (a). Each S/H amplifier catches a motor current just before a switching instance, and a differential amplifier calculates time difference of the motor current, i.e. $\Delta \boldsymbol{i}_k$, during an interval between two consecutive switchings. For example, the first and second S/H amplifiers from the top of Fig. 5 can sample i_α at the start and end points of an interval of $\boldsymbol{V}_1$, so that the top differential amplifier can calculate $\Delta i_{1\alpha}$. Finally, we can get a digital signal of $\Delta \boldsymbol{i}_k$, using two 8-bit A/D converters, each of which has an 8-channel multiplexer. Since A/D conversion is done after the differential amplifier calculates the time difference, high-resolution A/D converters are not

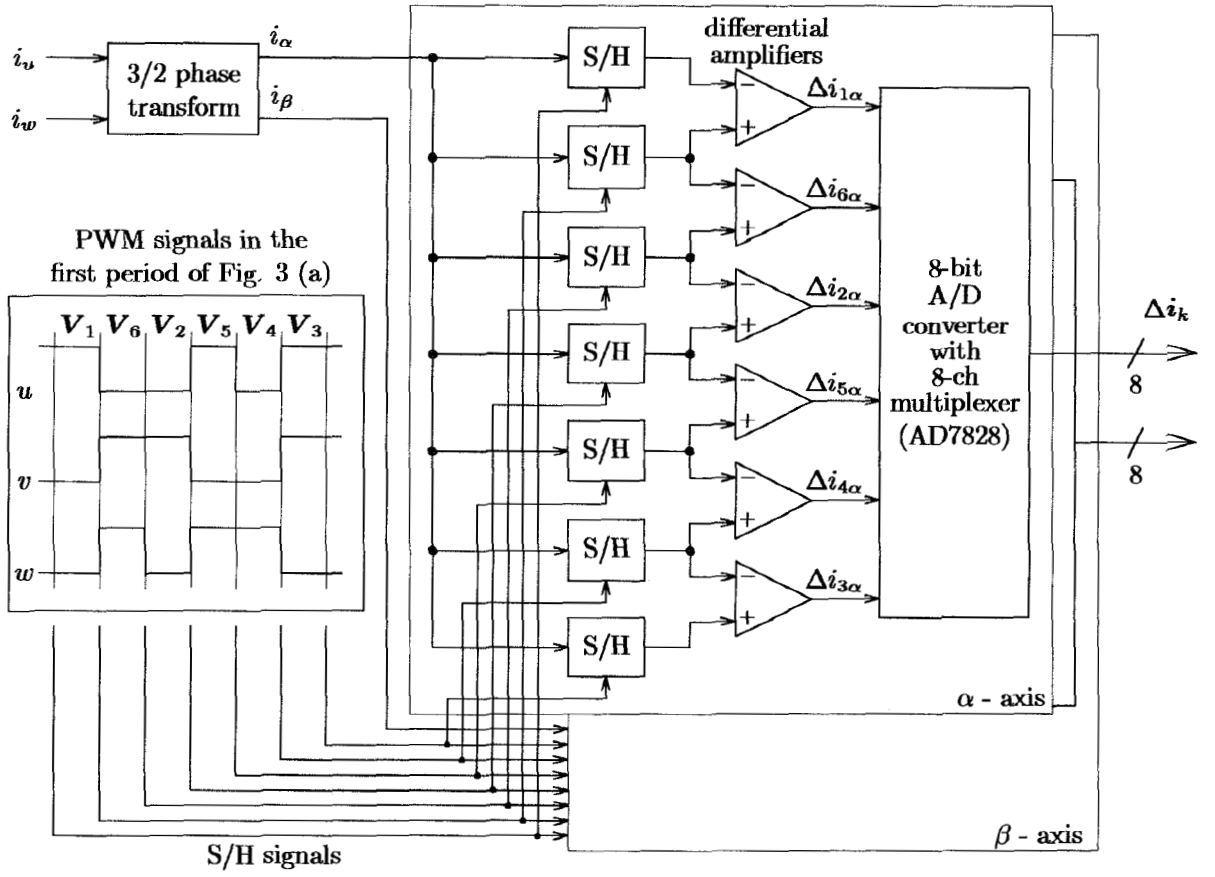

Fig. 5. Circuit configuration for extracting Δi_k.

necessary for the Δi_k extraction.

Fig. 6 shows waveforms of the three-phase motor currents at a standstill under no-load conditions. A triangle '∇' on the top of Fig. 6 indicates a moment of the current sampling. The experimental system detects Δi_k in the first period corresponding to Fig. 3 (a) and then estimates the rotor position in the second period. The sampling frequency of the position estimation, therefore, is 1.5 kHz. Each current includes a harmonic component varying linearly, but undesirable spike currents are superimposed on it. The spike current is a leakage current that escapes to earth through parasitic stray capacitance between windings and the frame of the IPM motor at any switching operation of the voltage-source PWM inverter [13]. Although the peak value of the leakage current reaches 2 A, current sampling just before a switching of the PWM inverter can ignore it so that the rotor position estimation is not influenced at all.

V. Experimental Results

Some experiments were carried out to examine performance of the constructed system. Static characteristics of position estimation were measured at a standstill under no-load conditions. In consequence of the experiment, it was confirmed that error in the estimated rotor position is less

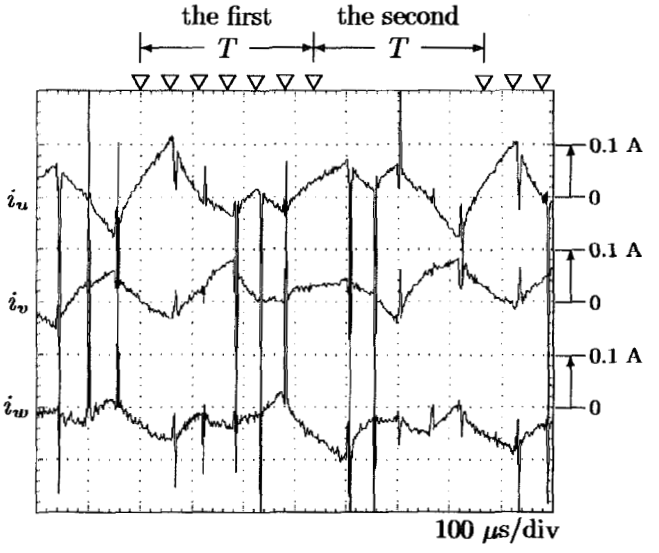

Fig. 6. Three-phase motor currents including harmonic components.

than 10 degrees in electrical angle [7].

A. Transient Response of Position Control

Fig. 7 shows a position response when the position reference θ^* was changed stepwise from 0 to 90 degrees under no-load conditions. All the waveforms were measured by two synchronized digital oscilloscopes (TDS 460, Tektronix) in *'Hi Res'* mode to remove the high frequency noise. Here, gains of the PI controller and the speed minor loop were adjusted so that the damping factor ζ, natural frequency ω_n, and time constant of the PI controller K_I/K_P, are 0.5, 20 rad/s, and 300 ms, respectively, taking into account the moment of inertia. These waveforms illustrate that the experimental system provides good position control performance of less than 100 ms rise time and 300 ms settling time. The approach to position estimation based on magnetic saliency makes it possible to implement position control in an IPM motor drive system without shaft-mounted position and speed sensors.

The estimated position agrees with the actual position even in a transient state, while the estimated speed contains some error. The reason is that a small amount of error in the estimated position is magnified by the calculation of time difference in the speed estimation. However, the estimated speed signal has enough ability to damp oscillation in position control. Fig. 8 shows a step response in the same conditions as Fig. 7 except for no speed minor loop, i.e. $G = 0$. An oscillation occurs after a step change in the position reference θ^*: The damping factor ζ of the oscillation approximates 0.05. The experimental result indicates that a minor loop based on the estimated speed makes a great contribution to stabilizing the position control.

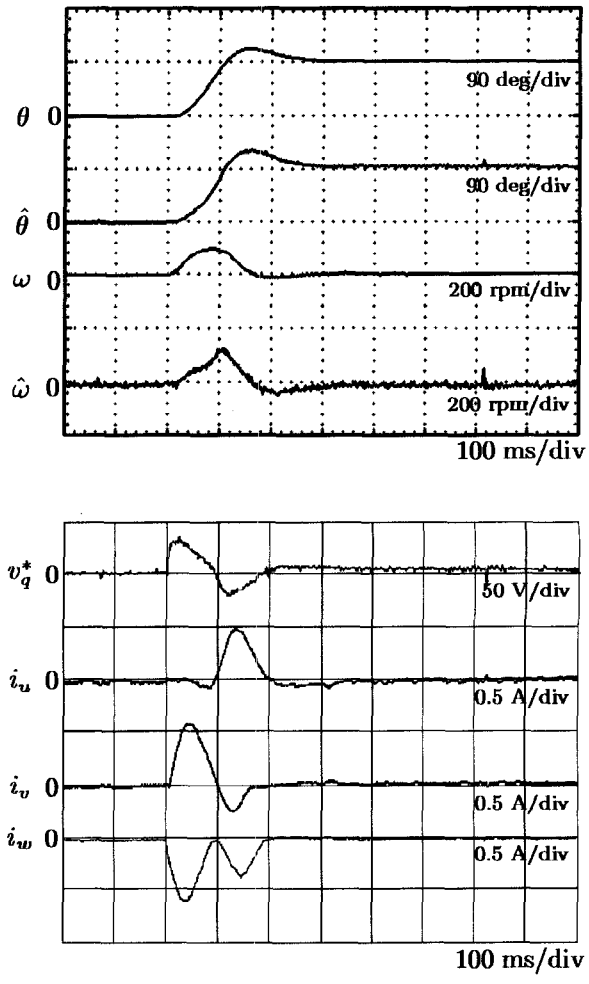

Fig. 7. Step responce in position control.

B. Electrical Lock of Motor Shaft: 'Servo-Lock'

Fig. 9 shows another transient response to a stepwise change in a mechanical load, keeping the position reference zero, that is, $\theta^* = 0$. A stepwise mechanical torque, corresponding to 60 % of the rated torque of the IPM motor, was applied to the motor shaft by a dc generator. The estimated position and speed waveforms conform to their actual waveforms even in a transient state. The step torque moved the rotor position immediately by 40 degrees, but the position control loop returned it to the original position after 1 s. This demonstrates that the experimental system implemented with the real-time position estimation method provides a 'servo-lock,' such that the position control loop can lock the motor shaft electrically even when a mechanical torque is loaded.

VI. Conclusion

This paper has dealt with a position control system of a position-sensorless IPM motor drive which is characterized by real-time rotor position estimation based on magnetic saliency. A motor inductance matrix including the rotor position information is determined from the motor current harmonics caused by PWM operation at every PWM period at a standstill and a low speed, without injecting any

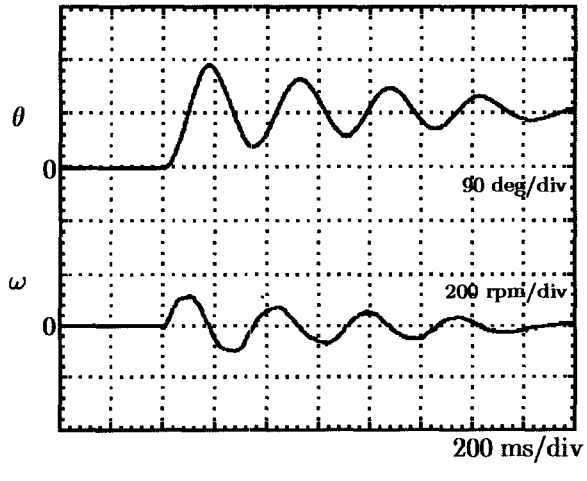

Fig. 8. Step response in position control without speed minor loop.

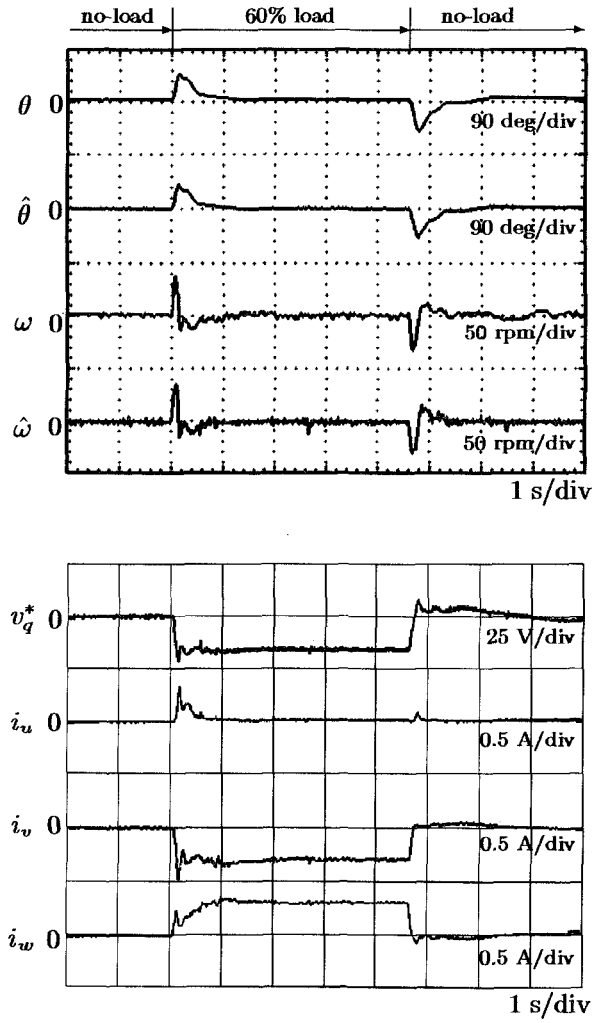

Fig. 9. Transient response to a step change in a mechanical load.

extra signal into the motor current or voltage. The estimation algorithm was implemented into a digital controller using a DSP, and an experimental position control system consisting of an IPM motor (100 W) and a voltage-source PWM inverter was made up and tested. As a result, experimental results demonstrate that the experimental system has good position control performance, with a position response of 20 rad/s and a settling time of 300 ms, and provides a 'servo-lock,' i.e. electrically locking the loaded motor shaft.

References

[1] K. Iizuka, H. Uzuhashi, M. Kano, T. Endo and K. Mori: "Microcomputer Control for Sensorless Brushless Motor," *IEEE Trans. on Industry Applications*, Vol. IA-21, No. 4, pp.595–601, May/June, 1985.

[2] S. Ogasawara and H. Akagi: "An Approach to Position Sensorless Drive for Brushless dc Motors," *IEEE Trans. on Industry Applications*, Vol. IA-27, No. 5, pp. 928–933, Sep./Oct., 1991.

[3] N. Matsui and T. Takeshita: "A Novel Starting Method of Sensorless Salient-Pole Brushless Motor," *IEEE/IAS Annual Meeting*, pp. 386–392, 1994.

[4] P. L. Jansen and R. D. Lorenz: "Transducerless Position and Velocity Estimation in Induction and Salient AC Machines," *IEEE/IAS Annual Meeting*, pp. 488–495, 1994.

[5] P. L. Jansen, M. J. Corley and R. D. Lorenz: " Flux, Position, and Velocity Estimation in AC Machines at Zero and Low Speed via Tracking of High Frequency Saliency," *EPE'95 Sevilla*, Vol. 3, pp. 154–159, 1995.

[6] S. Kondo, A. Takahashi and T. Nishida: "Armature Current Locus Based Estimation Method of Rotor Position of Permanent Magnet Synchronous Motor without Mechanical Sensor," *IEEE/IAS Annual Meeting*, pp. 55–60, 1995.

[7] S. Ogasawara and H. Akagi: "An Approach to Real-Time Position Estimation at Zero and Low Speed for a PM Motor Based on Saliency," *IEEE/IAS Annual Meeting*, pp. 29–35, 1996.

[8] A. B. Kulkarni and M.Ehsani: "A Novel Position Sensor Elimination Technique for the Interior Permanent-Magnet Synchronous Motor Drive," *IEEE Trans. on Industry Applications*, Vol. 28, No. 1, pp. 144–150, Jan./Feb., 1992.

[9] T. Matsuo and T. A. Lipo: "Rotor Position Detection Scheme for Synchronous Reluctance Motor Based on Current Measurements, " *IEEE Trans. on Industry Applications*, Vol. 31, No. 4, pp. 860–868, Jul./Aug., 1995.

[10] S. Ogasawara, H. Akagi and A. Nabae: "A Novel PWM scheme of Voltage Source Inverters Based on Space Vector Theory," *Archiv für Elektrotechnik*, Vol. 74, pp. 33-41, 1990.

[11] S.Wolfram: "Mathematica: A System for Doing Mathematics by Computer —Second Edition—," Addison-Wesley, 1991.

[12] J. J. Di Stefano, A.R. Stubberud, and I. J. Williams, *Feedback and Control Systems*, New York: McGraw-Hill, 1976.

[13] S. Ogasawara and H. Akagi: "Modeling and Damping of High-Frequency Leakage Currents in PWM Inverter-Fed AC Motor Drive Systems," *IEEE Trans. on Industry Applications*, Vol. IA-32, No. 5, pp. 1105–1114, Sep./Oct., 1996.